# Quantum distance and the Euler number index of the Bloch band in a one-dimensional spin model

Yu-Quan Ma*
*School of Applied Science, Beijing Information Science and Technology University, Beijing 100192, China*
(Dated: October 24, 2014)

We study the Riemannian metric and the Euler characteristic number of the Bloch band in a one-dimensional spin model with multi-site spins exchange interactions. The Euler number of the Bloch band originates from the Gauss-Bonnet theorem on the topological characterization of the closed Bloch states manifold in the first Brillouin zone. We study this approach analytically in a transverse field XY spin chain with three-site spin coupled interactions. We define a class of cyclic quantum distance on the Bloch band and on the ground state, respectively, as a local characterization for quantum phase transitions. Specifically, we give a general formula for the Euler number by means of the Berry curvature in the case of two-band models, which reveals its essential relation to the first Chern number of the band insulators. Finally, we show that the ferromagnetic-paramagnetic phases transition in zero-temperature can be distinguished by the Euler number of the Bloch band.

PACS numbers: 03.65.Vf, 73.43.Nq, 75.10.Pq, 05.70.Jk

arXiv:1403.2035v3 [cond-mat.str-el] 23 Oct 2014

## I. INTRODUCTION

The topological nature of quantum states has become a key ingredient in understanding the novel quantum phases of condensed-matter systems in low temperatures. Since the discovery of the Berry phase as a geometric phase picked up from the cyclic adiabatic evolutions of the Hamiltonian eigenstate and its holonomy interpretation on the $U(1)$ line bundle with parallel transport, many important findings on the topological nature of the quantum matter have come into physics, i.e., the quantized Hall conductance [1–3], adiabatic pumping [4, 5], topological insulators and superconductivity [6–10], and recently the fractional Chern insulators in flat bands [11–13].

In recent years, lots of attention has been attracted into understanding the quantum phase transitions (QPTs) [14–16] from the quantum information and the Hilbert space geometry aspects [17, 18]. Essentially, a QPT is the result of the competing ground-state phases driven by the quantum fluctuations, which can be witnessed by some qualitative changes of the ground-state properties, i.e., quantum entanglement [19–23], entanglement entropy [24, 25], quantum discord [26–28], quantum fidelity and the fidelity susceptibility [29–38], the Berry phase [39–49], and the quantum geometric tensor [50–58].

The ground-state geometric tensor, as an intrinsic metric on the ground-state complex manifold, is naturally expected to shed some light on the geometric characterization of QPTs. Mathematically, the quantum geometric tensor, also called the Fubini-Study metric, is a Hermitian metric on the complex projective space of the quantum states. Physically, the (non-Abelian) geometric tensor originates from defining a local $U(n)$ gauge invariant quantum distance between two states in a parameterized Hilbert space [55]. The quantum geometric tensor brings a Riemannian structure to the parameterized quantum states, where the corresponding Riemannian metric is given by the real part of the geometric tensor. Meanwhile, its imaginary part was later found to be just the Berry curvature (up to a constant coefficient). Specifically, the ground-state geometric tensor provides a unified mechanism from the aspect of information-geometry to understand the critical behaviors in quantum many-body systems.

Recently, a direct measurement of the Zak phase [59], as a Berry phase of a 1D Bloch band, has been achieved in one-dimensional (1D) optical lattices [60]. For the geometric tensor of the Bloch band, some interesting measurable consequences have been proposed by relating the geometric tensor of band insulators to the current noise spectrum [58]. A more interesting question is whether there exists some topological characterization related to the Riemannian metric of the Bloch bands? Very recently, a topological Euler number of the Bloch band was proposed to distinguish nontrivial topological phases in gapped free fermionic systems. This fact was pointed out in our previous work [61] and later by Kolodrubetz et. al [62].

In this work, we study the local and topological properties of the Bloch band in a 1D transverse field XY spin-1/2 model with three-site spin interactions. The system exhibits a nonzero transverse magnetization at the zero transverse field due to its multi-site spins exchange interactions. In order to obtain a well-defined geometric tensor in the crystal momentum space, we introduce an extra 1D parameter space by subjecting the spin system to a local gauge transformation, which in fact puts the Hamiltonian of the system on a torus $T^2$ in a 1+1D crystal momentum space without changing its energy spectrum. By using of the quantum Riemannian metric on the Bloch states manifold, we introduce a class of cyclic quantum distance as a local characterization for quantum phase transitions. Particularly, we derive the Euler

*Electronic address: mayuquan@iphy.ac.cn

characteristic number of the Bloch band analytically via the Gauss-Bonnet theorem on the Bloch states manifold in the first Brillouin zone. A general formula for the Euler number is obtained by means of the Berry curvature in the case of two-band models, which also reveals its relation to the first Chern number of the band insulators. Finally, we show that the ferromagnetic and paramagnetic quantum phase transitions can be distinguished by the different Euler numbers of the Bloch band.

## II. THE MODEL

We consider a 1D anisotropic XY spin-1/2 model with three-site spin exchange interactions in a transverse field. This spin model exhibits a nonzero transverse magnetization at the zero transverse field due to its multiple sites spin coupling and shows a rich ground-state phase diagram [63–66]. The Hamiltonian reads

$$\begin{aligned} H_{\mathrm{S}} &= \sum_{l\in N}^{\mathrm{PBC}} -(1+\gamma)\, S_l^x S_{l+1}^x - (1-\gamma)\, S_l^y S_{l+1}^y \\ &\quad -2\delta\left(S_{l-1}^x S_l^z S_{l+1}^x + S_{l-1}^y S_l^z S_{l+1}^y\right) - hS_l^z, \quad (1) \end{aligned}$$

where $S_l^\alpha$ $(\alpha = x, y, z; l \in N)$ is the Pauli operator on the local site $l$, $N$ denotes the total number of the sites, $\gamma$ is the anisotropy parameter in the in-plane interaction, $\delta$ denotes the three-site XZX+YZY type spins exchange interactions, $h$ is the transverse magnetic field, and the periodic boundary condition (PBC) has been imposed on this model.

Here we will show that the quantum critical points of the system can be witnessed by some local geometric characterization, i.e., the Riemannian metric on the Bloch band, and some partial derivative of the ground-state quantum distance. Particularly, we show that the zero-temperature phases diagram of the system can be marked by a nontrivial topological Euler number index of the Bloch band in the crystal momentum space.

In order to investigate the ground-state geometric tensor for the system, we need to define the metric tensor on a 2D parameter space. This can be achieved by subjecting the system to a local gauge transformation $H_{\mathrm{S}}(\varphi) = g(\varphi)H_{\mathrm{S}}g(\varphi)^\dagger$ by a twist operator $g(\varphi) = \prod_l e^{i\varphi S_l^z}$, which makes the system a rotation on the spin along the $z$-direction. It can be verified that $H_{\mathrm{S}}(\varphi)$ is $\pi$ periodic in $\varphi$ because the quadratic form about the $x$ and $y$ axes appears symmetric in the Hamiltonian. Considering the unitarity of the twist operator $g(\varphi)$, the critical behavior and energy spectrum of the system are obviously parameter $\varphi$ independent.

The spin Hamiltonian $H_{\mathrm{S}}(\varphi)$ can be mapped exactly on a spinless fermion Hamiltonian $H_{\mathrm{F}}(\varphi)$ by the Jordan-Wigner transformation $a_l = \prod_{m=1}^{l-1}(-2S_m^z)\, S_l^-$, $a_l^\dagger = \prod_{m=1}^{l-1}(-2S_m^z)\, S_l^+$, where $S_l^\pm = S_l^x \pm iS_l^x$ denote the spin ladder operators and $a_l$, $a_l^\dagger$ are the corresponding Fermion annihilation and creation operators, respectively, on the local site $l$. After applying a Fourier transformation $a_l = \frac{1}{\sqrt{N}}\sum_{k\in \mathrm{Bz}} e^{ikl}c_k$, we can rewrite the fermion Hamiltonian as

$$H_{\mathrm{F}}(\varphi) = \sum_{k\in \mathrm{Bz}} \Psi_{k,\varphi}^\dagger \left(\sum_{\alpha=1}^{3} d_\alpha(k,\varphi)\,\sigma^\alpha\right)\Psi_{k,\varphi}, \quad (2)$$

where $d_1(k,\varphi) = \frac{1}{2}\gamma \sin k \sin 2\varphi$, $d_2(k,\varphi) = \frac{1}{2}\gamma \sin k \cos 2\varphi$, $d_3(k,\varphi) = \frac{1}{2}(-h + \delta\cos 2k - \cos k)$, $\Psi_{k,\varphi}^\dagger := \left(c_k^\dagger, c_{-k}\right)$ and $\sigma^\alpha$ denotes the the Pauli matrices, represent the pseudo-spin degree of freedom.

The Bloch wave function can be expressed as

$$u_\pm(k,\varphi) = \frac{1}{\sqrt{2d\left(d \mp d_3(k,\varphi)\right)}}\begin{pmatrix} d_1(k,\varphi) - id_2(k,\varphi) \\ \pm d - d_3(k,\varphi)\end{pmatrix}, \quad (3)$$

and the corresponding energy spectrum is $E_\pm(k) = \pm d$, where $d := \sqrt{\sum_{\alpha=1}^{3} d_\alpha^2(k,\varphi)}$. The Hamiltonian can be diagonalized as $H(\varphi) = \sum_{k\in \mathrm{Bz}} E_+(k)\alpha_{k,\varphi}^\dagger\alpha_{k,\varphi} + E_-(k)\beta_{k,\varphi}^\dagger\beta_{k,\varphi}$, and the $\varphi$ parameterized ground-state $|e(\varphi)\rangle$ is the filled fermion sea

$$|e(\varphi)\rangle = \prod_{k>0} \beta_{-k,\varphi}^\dagger \beta_{k,\varphi}^\dagger |0\rangle, \quad (4)$$

where the quasi-particle operators $\alpha_{k,\varphi} = \left[u(\varphi,k)_+\right]^\dagger \Psi_{k,\varphi}$ and $\beta_{k,\varphi} = \left[u(\varphi,k)_-\right]^\dagger \Psi_{k,\varphi}$. Note that the Bloch Hamiltonian $\mathcal{H}(k,\varphi) := \sum_{\alpha=1}^{3} d_\alpha(k,\varphi)\,\sigma^\alpha$ is period $\pi$ on the parameter $\varphi$, that is $\mathcal{H}(k,0) = \mathcal{H}(k,\pi)$. On the other hand, the Bloch Hamiltonian $\mathcal{H}(k,\varphi)$ can be regarded periodic in the Brillouin zone up to a gauge transformation $\mathcal{H}(k+G,\varphi) = e^{-iG\cdot r}\mathcal{H}(k,\varphi)e^{iG\cdot r}$, where $G$, and $r$ are the reciprocal lattice vector and position vector, respectively. Note that in a lattice model, here the gauge factor is just identically equal to 1, and we have $\mathcal{H}(k+G,\varphi) = \mathcal{H}(k,\varphi)$. Hence, the Bloch Hamiltonian $\mathcal{H}(k,\varphi)$ has been put on a torus $T^2$ in a 1+1D crystal momentum space.

## III. GEOMETRIC TENSOR ON THE BLOCH STATES MANIFOLD

To begin with, we give a brief discussion on the quantum geometric tensor of the Bloch band. The quantum geometric tensor of the Bloch band can be derived naturally from a gauge invariant distance between two Bloch states on the $U(1)$ line bundle induced by the quantum adiabatic evolution of the Bloch state $|u_n(k)\rangle$ of the $n$-th filled band. The gauge invariant quantum distance between two states $|u_n(k+\delta k)\rangle$ and $|u_n(k)\rangle$ is given by

$$dS^2 = \sum_{\mu,\upsilon} \langle\partial_\mu u_n|\left[\mathbf{1} - \mathcal{P}_n\right]|\partial_\nu u_n\rangle\, dk^\mu dk^\upsilon, \quad (5)$$

where $\mathcal{P}_n = |u_n\rangle\langle u_n|$ is the projection operator, and $\mu,\nu$ denote the components $k^\mu$ and $k^\nu$, respectively. The quantum geometric tensor is given by

$$Q_{\mu\nu} = \langle\partial_\mu u_n|\left[\mathbf{1}-\mathcal{P}_n\right]|\partial_\nu u_n\rangle\,. \tag{6}$$

The underlying mechanism for the quantum distance can be understood as follows: The term $|\partial_\mu u_n\rangle$ can be decomposed in the complete Hilbert space as $|\partial_\mu u_n\rangle = |D_\mu u_n\rangle + [\mathbf{1}-\mathcal{P}_n]|\partial_\mu u_n\rangle$, where $|D_\mu u_n\rangle = \mathcal{P}_n|\partial_\mu u_n\rangle$ is the covariant derivative of $|u_n\rangle$ on the line bundle. Under the condition of the quantum adiabatic evolution, the evolution of $|u_n(k)\rangle$ to $|u_n(k+\delta k)\rangle$ will undergo a parallel transport, that is $|D_\mu u_n(k)\rangle = 0$, which will lead to a gauge invariant quantum distance as Eq. (5). The geometric tensor Eq. (6) can be rewritten as $Q_{\mu\nu} = \mathcal{G}_{\mu\nu} - i\mathcal{F}_{\mu\nu}/2$, where $\mathcal{G}_{\mu\nu}$ :=Re$Q_{\mu\nu}$ can be verified as a Riemannian metric, which establishes a Riemannian manifold of the Bloch states. It can be verified that the quantum distance is only depend on the real part of the quantum geometric tensor, that is $dS^2 = \sum_{\mu,\upsilon}\mathcal{G}_{\mu\nu}dk^\mu dk^\upsilon$, because the term $\mathcal{F}_{\mu\nu} := -2\text{Im}Q_{\mu\nu}$ is canceled out in the summation of the distance due to its antisymmetry. However, the term $\mathcal{F}_{\mu\nu}$ can be associated to a two-form $\mathcal{F} = \sum_{\mu,\upsilon}\mathcal{F}_{\mu\nu}dk^\mu\wedge dk^\nu$, which is nothing but the Berry curvature.

### A. Riemannian metric and the cyclic quantum distance of the Bloch band

The Riemannian metric of the Bloch band is given by $\mathcal{G}_{\mu\nu} = \text{Re}Q_{\mu\nu}$, where the geometric tensor $Q_{\mu\nu}$ can be obtained by substituting Eq. (3) to Eq. (6), and it can be verified that this metric $\mathcal{G}$ is given by the following diagonalized form [67]

$$dS^2 = \mathcal{G}_{kk}dk^2 + \mathcal{G}_{\varphi\varphi}d\varphi^2, \tag{7}$$

with

$$\begin{aligned}\mathcal{G}_{kk} &= \left[\frac{1}{2}\frac{\gamma+\gamma(h-2\delta+\delta\cos 2k)\cos k}{(h+\cos k-\delta\cos 2k)^2+\gamma^2\sin^2 k}\right]^2,\\ \mathcal{G}_{\varphi\varphi} &= \frac{\gamma^2\sin^2 k}{(h+\cos k-\delta\cos 2k)^2+\gamma^2\sin^2 k}.\end{aligned} \tag{8}$$

The metric $\mathcal{G}$ is obviously independent on the parameter $\varphi$ because of its $U(1)$ gauge invariance on the twist operator.

In Fig. 1, we show that the trace of the Riemannian metric as a function of the external field $h$ and the crystal momentum $k$ with different three-site spins coupled parameters and the anisotropy parameters. As we expect, the singularity regions of the metric will appear when the external field $h$ is close to the quantum critical points. We define a cyclic quantum distance on the Bloch band from $(0,-\pi)$ to $(\pi,\pi)$ in the extended first Brillouin zone (the inset in Fig.2), where the parameter path of the integral loop $C$ is $\varphi = k/2+\pi/2$, $(k\in 1\text{Bz})$,

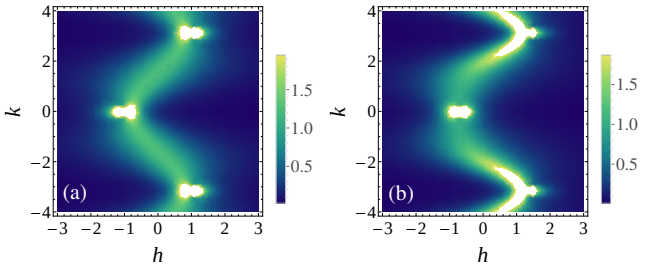


FIG. 1: (color online) The trace of the Riemannian metric Tr$\mathcal{G}$ as a function of the external field $h$ and the crystal momentum $k$ with the fixed Hamiltonian parameters: (a) the three-site spins exchange interactions $\delta = 0$ and the anisotropy parameter $\gamma = 1$; (b) $\delta = 0.3$ and $\gamma = 0.9$.

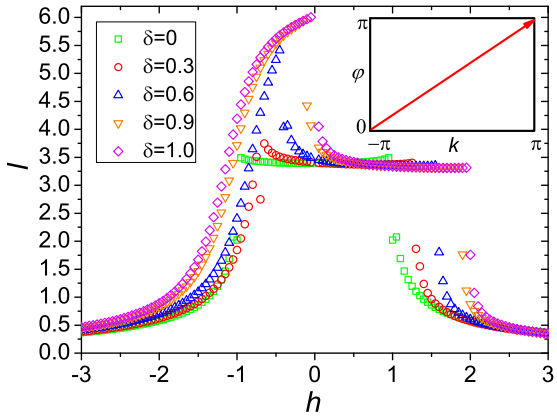


FIG. 2: (color online) The cyclic quantum distance $l$ of the Bloch band as a function of $h$, with the fixed anisotropy parameter $\gamma = 1/3$ and different three-site spins coupled coefficients $\delta$, where the integral path is along the diagonal line in the extended Brillouin zone (inset).

which is just the diagonal line in the extended Brillouin zone.

The cyclic quantum distance $l$ of the Bloch band is given by

$$l = \oint_C\sqrt{\mathcal{G}_{kk}dk^2+\mathcal{G}_{\varphi\varphi}d\varphi^2} = \int_{-\pi}^{\pi}\sqrt{\mathcal{G}_{kk}+\frac{1}{4}\mathcal{G}_{\varphi\varphi}}dk. \tag{9}$$

where the Riemannian metric $\mathcal{G}_{kk}$ and $\mathcal{G}_{\varphi\varphi}$ are given by Eq. (8). As shown in Fig. 2, we calculate the cyclic quantum distance $l$ as a function of $h$, with the fixed anisotropy parameter $\gamma = 1/3$ and different three-site spins coupled coefficients $\delta$. The singularity points on the cyclic quantum distance are just corresponding to the quantum transition points $|\delta-1|$ and $|\delta+1|$.

In Fig. 3, we plot the the cyclic quantum distance $l$ with the fixed three-site spins coupled coefficients $\delta = 0.3$ and different anisotropy parameters $\gamma$. It can be seen that the value of the anisotropy parameter $\gamma$ does not

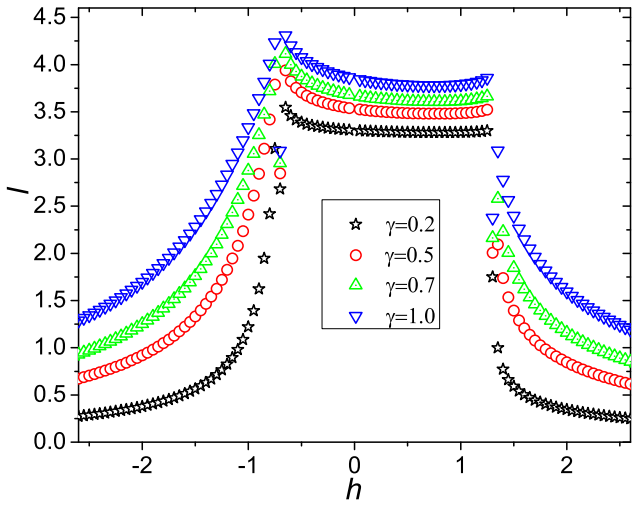


FIG. 3: (color online) The cyclic quantum distance $l$ of the Bloch band as a function of $h$, with the fixed three-site spins coupled coefficient $\delta = 0.3$ and different anisotropy parameters $\gamma$.

affect the critical point but makes the cyclic quantum distance $l$ approach zero more quickly in the paramagnetic phase.

### B. Cyclic quantum distance of the ground state

It is worth noting that the metric component $\mathcal{G}_{\varphi\varphi}$ on the Bloch band is closely related to the ground-state quantum distance in the parameter $\varphi$ space. In fact, the ground state $|e(\varphi)\rangle$ is $\pi$ periodic in the parameter $\varphi$. In the condition of the large sites limit $N \to \infty$, a cyclic ground-state distance $l_e$ can be defined along the $\varphi$ -ring as

$$\begin{aligned} l_e &= \int_0^{\pi} \sqrt{\langle \partial_\varphi e(\varphi)| \left[\mathbf{1} - \mathcal{P}_e\right] |\partial_\varphi e(\varphi)\rangle} d\varphi \\ &= \frac{1}{2\pi} \iint \sqrt{\mathcal{G}_{\varphi\varphi}} dk d\varphi, \end{aligned} \tag{10}$$

where $\mathcal{P}_e = |e(\varphi)\rangle \langle e(\varphi)|$ denotes the ground-state projection operator and the Eqs. (3) and (4) have been used in the intermediate steps. Note that the result in Eq. (10) is general, which only relates to the metric $\mathcal{G}_{\varphi\varphi}$ on the Bloch band and the concrete expression of the ground state is not required.

In Fig. 4 (a), we show the derivative of the cyclic ground-state distance with respect to the external field $h$ under different lattice sizes $N$, where the Hamiltonian parameters $\gamma = 0.7$ and $\delta = 0.3$. As shown in Fig. 4 (b), we can see that the positions of the maximum points of the derivative $dl_e/dh$, with the increasing of the lattice sizes, tend as $N^{-1.0074}$ and $N^{-0.7122}$ to the critical points $h_c = 0.7$ and $h_c = 1.3$, respectively.

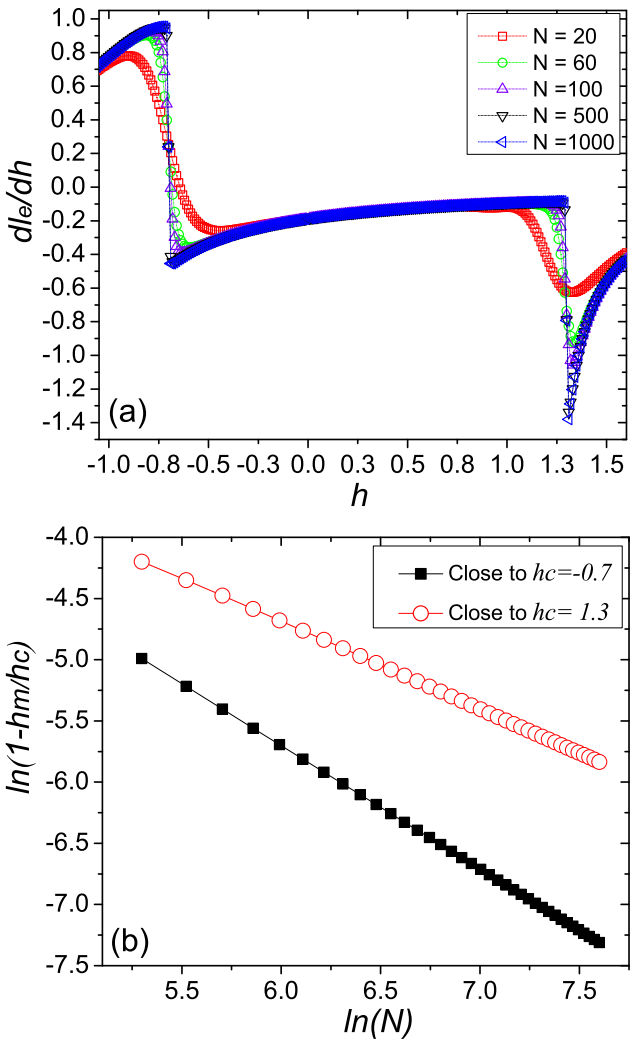


FIG. 4: (color online) (a) The derivative of the cyclic ground-state distance $dl_e/dh$ with different lattice sizes $N$, where the Hamiltonian parameters $\gamma = 0.7$ and $\delta = 0.3$; (b) with the increasing of the lattice sizes, the positions of the maximum points of $dl_e/dh$ tend as $N^{-1.0074}$ and $N^{-0.7122}$ to the critical points $h_c = 0.7$ and $h_c = 1.3$, respectively.

## IV. THE EULER CHARACTERISTIC NUMBER OF THE BLOCH BAND

What is more interesting is that the Euler characteristic number of the Bloch band can be derived from the Gauss-Bonnet theorem on the Bloch states manifold established by the Riemannian metric $\mathcal{G}^{(n)}_{\mu\nu}$. The Euler characteristic number $\chi$ of all occupied bands can be generalized written by (see Ref. [61])

$$\chi = \frac{1}{4\pi} \sum_n \iint_{1\mathrm{Bz}} \mathcal{R}^{(n)} \sqrt{\det \mathcal{G}^{(n)}_{\mu\nu}} dk^\mu dk^\nu, \tag{11}$$

where the $\mathcal{R}^{(n)}$ is the Ricci scalar curvature associate to the Bloch state $|u_n(k)\rangle$ of the $n$-th Bloch band. The

Ricci scalar curvature $\mathcal{R}$ can be calculated by using the standard steps: $\mathcal{R} = \mathcal{G}^{ab}R_{acb}^{\cdots c}$, where the Riemannian curvature tensor

$$R_{abc}^{\cdots d} = \partial_b\Gamma_{ac}^d - \partial_a\Gamma_{bc}^d + \Gamma_{ac}^e\Gamma_{be}^d - \Gamma_{bc}^e\Gamma_{ae}^d, \tag{12}$$

and the Levi-Cività connection $\Gamma_{bc}^a$ can be calculated by

$$\Gamma_{bc}^a = \frac{1}{2}\mathcal{G}^{ad}\left(\partial_b\mathcal{G}_{dc} + \partial_c\mathcal{G}_{bd} - \partial_d\mathcal{G}_{cb}\right). \tag{13}$$

The Riemannian metric $\mathcal{G}$ of the Bloch band is given by Eq. (8), and its contravariant component can be easily obtained as $\mathcal{G}^{kk} = 1/\mathcal{G}_{kk}$, and $\mathcal{G}^{\varphi\varphi} = 1/\mathcal{G}_{\varphi\varphi}$. By using Eqs. (8) and (13), we can obtain all of the non-zero connections as

$$\begin{aligned}
\Gamma_{k\varphi}^{\varphi} &= \Gamma_{\varphi k}^{\varphi} \\
&= \frac{\left(B-\gamma^2\cos k\right)\sin k - 2\delta B\sin 2k}{B^2+\gamma^2\sin^2 k} \\
&\quad + \cot k, \\
\Gamma_{kk}^{k} &= 2\frac{\left(B-\gamma^2\cos k\right)\sin k - 2\delta B\sin 2k}{B^2+\gamma^2\sin^2 k} \\
&\quad - \frac{(h+3\delta\cos 2k)\sin k}{1+A\cos k}, \\
\Gamma_{\varphi\varphi}^{k} &= -\frac{4B\sin k}{1+A\cos k},
\end{aligned} \tag{14}$$

with

$$\begin{aligned}
A &= h + \delta\cos 2k - 2\delta, \\
B &= h - \delta\cos 2k + \cos k.
\end{aligned} \tag{15}$$

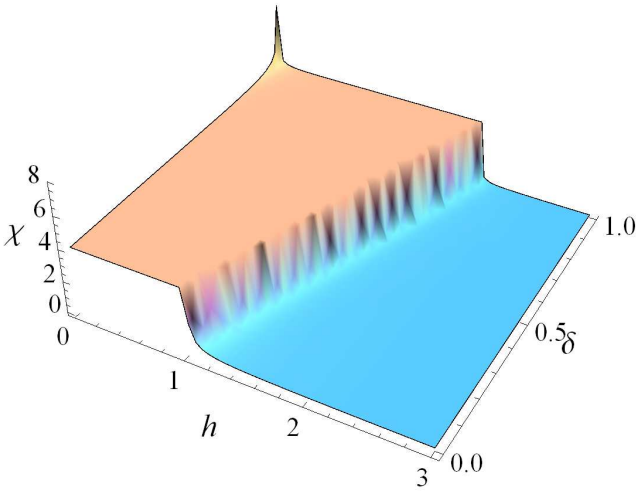


FIG. 5: (color online) The Euler number $\chi$ of the Bloch band as a function of the external field $h$ and three-site spins coupled coefficients $\delta$. The ferromagnetic phase in this model can be marked by a nontrivial Euler number $\chi = 4$, and the Euler number $\chi \to 0$ quickly with the increasing of the external field $h$ in the paramagnetic phase.

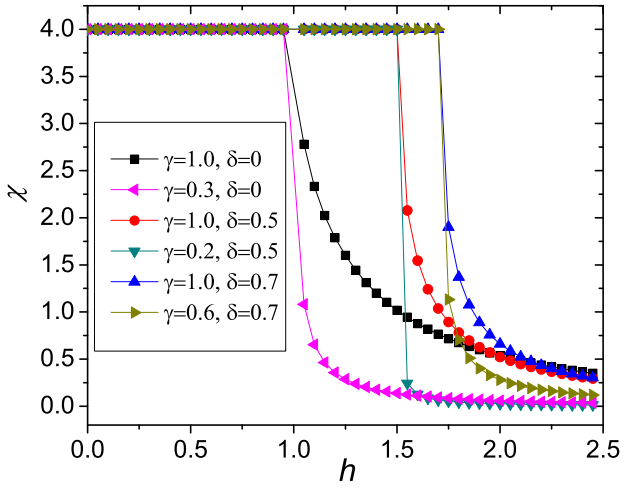


FIG. 6: (color online) The Euler number $\chi$ with several groups of the anisotropy parameter $\gamma$ and three-site spins coupled coefficients $\delta$.

The Euler characteristic number $\chi$ is a topological invariant and equals to $2\,(1-g)$ with genus $g$ for a closed smooth manifold. Note that the Bloch band of the model forms a 2D closed Riemannian manifold in the first Brillouin zone, and then the Euler characteristic number can be calculated conveniently by the Gauss-Bonnet theorem $\chi = \frac{1}{2\pi}\int_{1\mathrm{Bz}}\mathcal{K}dA$, where $\mathcal{K} = R_{k\varphi\varphi k}/\det\mathcal{G}_{k\varphi}$ is the Gauss curvature, which just equals to the half of the Ricci scalar curvature $\mathcal{R}$, and the covariant Riemannian curvature tensor $R_{abcd} := R_{abc}^{\cdots e}\mathcal{G}_{ed}$ have only one substantial component $R_{k\varphi k\varphi}$, and $dA = \sqrt{\det\mathcal{G}_{k\varphi}}dkd\varphi$ denotes the area measure.

The direct calculation of the $R_{k\varphi k\varphi}$ and $\sqrt{\det\mathcal{G}_{k\varphi}}$ are tedious, however, it can be verified that there exists a general relation in a generalized two-band Hamiltonian on a 2D manifold as $R_{k\varphi k\varphi} = 4\det\mathcal{G}_{k\varphi}$ and $\det\mathcal{G}_{k\varphi} = \left(\frac{\hat{\boldsymbol{d}}\cdot\partial_k\hat{\boldsymbol{d}}\times\partial_\varphi\hat{\boldsymbol{d}}}{4}\right)^2$. That is to say that the Bloch band manifold is a curved surface with a constant Gauss curvature $\mathcal{K} = 4$. Finally, we can derive the Euler number of the Bloch band as

$$\begin{aligned}
\chi &= \frac{1}{2\pi}\int_{1\mathrm{Bz}}\mathcal{K}dA \\
&= \frac{1}{2\pi}\iint_{1\mathrm{Bz}}\left|\hat{\boldsymbol{d}}\cdot\partial_k\hat{\boldsymbol{d}}\times\partial_\varphi\hat{\boldsymbol{d}}\right|dkd\varphi,
\end{aligned} \tag{16}$$

where

$$\hat{\boldsymbol{d}}\cdot\partial_k\hat{\boldsymbol{d}}\times\partial_\varphi\hat{\boldsymbol{d}} = \frac{2\gamma^2\sin k + \gamma^2(h-2\delta+\delta\cos 2k)\sin 2k}{\left[(h+\cos k-\delta\cos 2k)^2+\gamma^2\sin^2 k\right]^{3/2}}. \tag{17}$$

As shown in Fig. 5, we plot the Euler number $\chi$ of the Bloch band as a function of the external field $h$ and three-site spins coupled coefficients $\delta$. In the ferromagnetic phase, the Bloch band is characterized by a nontrivial Euler number $\chi = 4$, whose topology is equivalent to

two unconnected spheres $S^2$; in the paramagnetic phase, the Euler number of the Bloch band $\chi \to 0$ quickly with the increasing of the external field $h$, whose topology is equivalent to a torus $T^2$. The effects of the anisotropy parameter $\gamma$ on the Euler number are shown in the Fig. 6. It can be seen that the Euler number is independent of $\gamma$ in the region of the ferromagnetic phase, but declines to 0 more quickly with the decreasing of $\gamma$ in the region of the paramagnetic phase.

Note that the Berry curvature of the Bloch band can be written as $\mathcal{F}_{k\varphi} = \frac{1}{2}\hat{\boldsymbol{d}} \cdot \partial_k \hat{\boldsymbol{d}} \times \partial_\varphi \hat{\boldsymbol{d}}$, so we can get a first Chern number index for the Bloch band as

$$C_1 = \frac{1}{4\pi} \iint_{1\mathrm{Bz}} \hat{\boldsymbol{d}} \cdot \partial_k \hat{\boldsymbol{d}} \times \partial_\varphi \hat{\boldsymbol{d}} \, dk d\varphi. \tag{18}$$

However, the Bloch Hamiltonian for this model $\mathcal{H}(k,\varphi) = \sum_{\alpha=1}^{3} d_\alpha(k,\varphi)\sigma^\alpha$ is time reversal invariant, i.e. $\mathcal{H}^*(-k,-\varphi) = \mathcal{H}(k,\varphi)$, so the Berry curvature $\mathcal{F}_{k\varphi}$ is odd with the crystal momentum $k$ (note $\mathcal{F}_{k\varphi}$ is not dependent on $\varphi$), and the first Chern number $C_1 \equiv 0$. In this case, the first Chern number can not serve as a sufficient index for the topology of the Bloch band in the time reversal invariant systems.

For an intuitive picture, the original 1D fermionic Hamiltonian without the twist operation is given by

$$H_{1D} = \sum_{k\in \mathrm{Bz}} \left(c_k^\dagger,\, c_{-k}\right) \mathcal{H}_{1\mathrm{D}}(k) \begin{pmatrix} c_k \\ c_{-k}^\dagger \end{pmatrix}, \tag{19}$$

where the Bloch Hamiltonian $\mathcal{H}_{1\mathrm{D}}(k) = \sum_{\alpha=1}^{3} d_\alpha(k)\sigma^\alpha$, with $d_1(k) = 0$, $d_2(k) = \frac{1}{2}\gamma \sin k$, $d_3(k) = \frac{1}{2}(-h + \delta\cos 2k - \cos k)$, can be verified to be time-reversal invariant because $\mathcal{H}_{1\mathrm{D}}^*(-k) = \mathcal{H}_{1\mathrm{D}}(k)$. Meanwhile, $\mathcal{H}_{1\mathrm{D}}(k)$ has a particle-hole symmetry $(\sigma^x K)\,\mathcal{H}_{1\mathrm{D}}(k)\,(\sigma^x K)^{-1} = -\mathcal{H}_{1\mathrm{D}}(-k)$ because $d_3(k)^* = d_3(-k)$, $d_1(k)^* = -d_1(-k)$ and $d_2(k)^* = -d_2(-k)$. As a result of the time-reversal and particle-hole symmetry, the Hamiltonian $\mathcal{H}_{1\mathrm{D}}(k)$ has also a chiral symmetry. Therefore, the 1D Hamiltonian $H_{1D}$ is in the BDI class. It has been shown that BDI class Hamiltonians in one dimension are classified by an integer $\mathbb{Z}$ topological invariant [68]. The $\mathbb{Z}$ number can be expressed as the winding number of the 2D vector $\boldsymbol{d}(k) = (d_2(k), d_3(k))$ around the gapless point $|\boldsymbol{d}(k)| = 0$ when $k$ runs across the first Brillouin zone. The winding number can be written as [69]

$$N_{\mathrm{BDI}} = \frac{1}{2\pi} \int_{-\pi}^{\pi} d\Phi(k), \tag{20}$$

where $\Phi(k) = \arctan[d_3(k)/d_2(k)]$ denotes the angle of the vector $\boldsymbol{d}(k)$. As shown in Fig. 7, we plot the vector $\boldsymbol{d}(k)$ with the Hamiltonian parameters $\delta = 0.7$, $\gamma = 1$ and different $h$. It can be seen clearly that the ferromagnetic phase and paramagnetic phase are topologically nonequivalent depending on whether or not the gapless point is enclosed within the the curve of $\boldsymbol{d}(k)$, and the quantum phase transitions occur at $h = \delta \pm 1$.

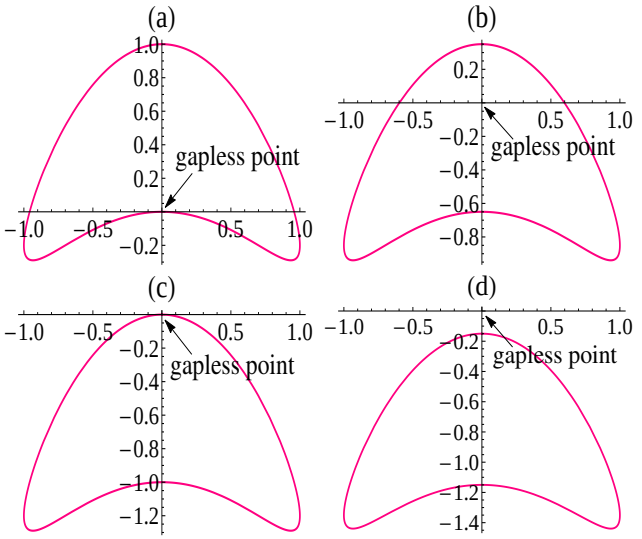


FIG. 7: (color online) The trajectories of the 2D vector $\boldsymbol{d}(k)$ with the Hamiltonian parameters $\delta = 0.7$, $\gamma = 1$ and (a) $h = -0.3$; (b) $h = 1$; (c) $h = 1.7$; (d) $h = 2$.

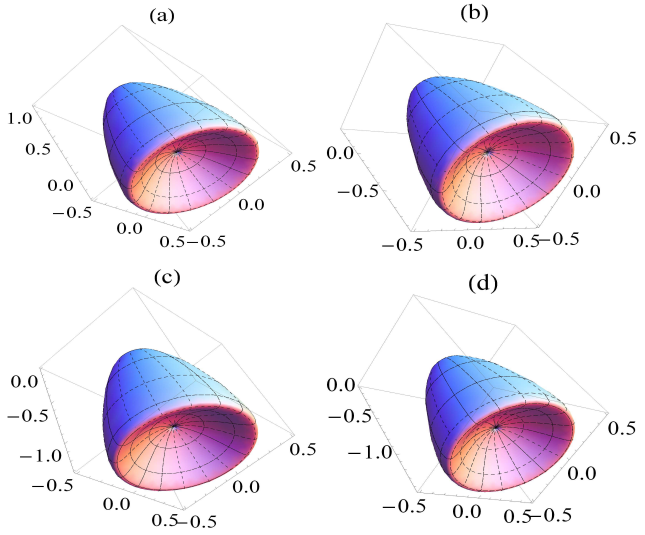


FIG. 8: (color online) The trajectories of the 3D vector $\boldsymbol{d}(k,\varphi)$ with the Hamiltonian parameters $\delta = 0.7$, $\gamma = 1$ and (a) $h = -0.3$; (b) $h = 1$; (c) $h = 1.7$; (d) $h = 2$.

In the Euler number approach, the 1D Hamiltonian has been extended to two dimensions by subjecting the system to a gauge transformation (see Eq. (2)), and meanwhile its energy spectrum remains unchanged. As a consequence, the 2D Bloch Hamiltonian $\mathcal{H}(k,\varphi)$ only remains time-reversal invariant, and then belongs to the symmetry class AI without a strong topological invariant in two dimensions.

However, it can be verified that there exists an intuitive topological connection between $\mathcal{H}(k,\varphi)$ and $\mathcal{H}_{1\mathrm{D}}(k)$. As

shown in Fig. 8, the trajectories of the vector $\boldsymbol{d}(k,\varphi)$ are corresponding to the rotation of the vector $\boldsymbol{d}(k)$ around the "$d_3$"-axis, and meanwhile, keeping the gapless point unchanged. As the same as the 1D case, the ferromagnetic phase and paramagnetic phase are topologically nonequivalent which can be characterized by whether or not the gapless point is enclosed by the closed surface of $\boldsymbol{d}(k,\varphi)$. Note that here the first Chern number can not provide an effective distinction because the Berry curvature is odd with $k$ in the time-reversal invariant Hamiltonian $\mathcal{H}(k,\varphi)$. However, we show that here the Euler number of the band can servers as an effective topological number as the replacement of the Chern number, because the Euler number can be expressed as the integral of the absolute value of the Berry curvature in the first Brillouin zone.

It also needs to be pointed out that the Euler number in the ferromagnetic phase is characterized by the even number $\chi = 4$ instead of $\chi = 2$. This is because the trajectories of the vector $\boldsymbol{d}(k,\varphi)$ can be split into two equal disjoint topological spheres $\boldsymbol{d}(k,\varphi)$ with $k \in [-\pi, 0]$, and $\boldsymbol{d}(k,\varphi)$ with $k \in [0,\pi]$ (see Fig. 9). Note that each of the topological spheres will contribute a Euler number 2 ($\chi = 2(1-g)$, with $g = 0$ for a topological sphere), and hence the two topological spheres will contribute the Euler number $\chi = 4$.

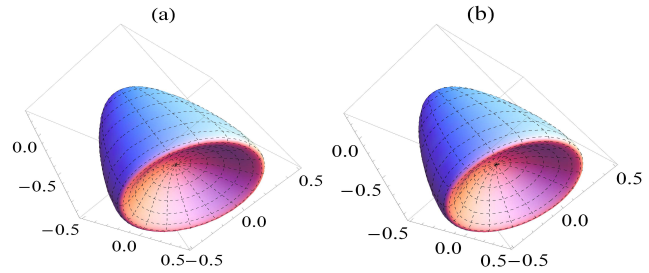


FIG. 9: (color online) The trajectories of the 3D vector $\boldsymbol{d}(k,\varphi)$ with the Hamiltonian parameters $\delta = 0.7$, $\gamma = 1$ and $h = 1$ can be split into two equal disjoint topological spheres (a) $\boldsymbol{d}(k,\varphi)$ with $k \in [-\pi, 0]$; and (b) $\boldsymbol{d}(k,\varphi)$ with $k \in [0,\pi]$.

For the measurable consequence, Neupert et. al. have recently shown that the quantum geometric tensor $Q_{\mu\nu}$ of the band can be measured by the current noise spectrum of the band insulators. In a two-band Hamiltonian, the current noise spectrum can be expressed by the $Q_{\mu\nu}$ of the band as (see Eq. (13) in Ref. [58])

$$S_{\mu\nu}(\omega) = -2\pi\omega^2 \int_{1\mathrm{Bz}} \frac{d^d\boldsymbol{k}}{\Omega_{\mathrm{Bz}}} \delta\left[\omega - E_+(\boldsymbol{k}) + E_-(\boldsymbol{k})\right] Q_{\mu\nu}(\boldsymbol{k}), \tag{21}$$

where $\Omega_{\mathrm{BZ}}$ denotes the volume of the Brillouin zone, $d$ denotes the dimension of the crystal momentum space, and

$$S_{\mu\nu}(\omega) := \int dt\ e^{-i\omega t} \langle 0|J_\mu(0)J_\nu(t)\,|0\rangle \tag{22}$$

is the spectral function of the current-current correlation. As shown by Marzari and Vanderbilt [70], the integral of the trace of the Riemannian metric over the Brillouin zone $\Omega_I = \int_{1\mathrm{Bz}} \frac{d^d\boldsymbol{k}}{\Omega_{\mathrm{Bz}}} \mathrm{Tr}\mathcal{G}$ is a gauge invariant measure of the delocalization or spread of the Wannier functions. Here, we would like to point out that the Euler number of the band, in the case of a 2D two-band Hamiltonian, can be reduced to a gauge invariant volume of the Brillouin zone as measured according to the metric $\mathcal{G}$ (see Eq. (16) ) and this volume can be topological invariant in the nontrivial topological phase.

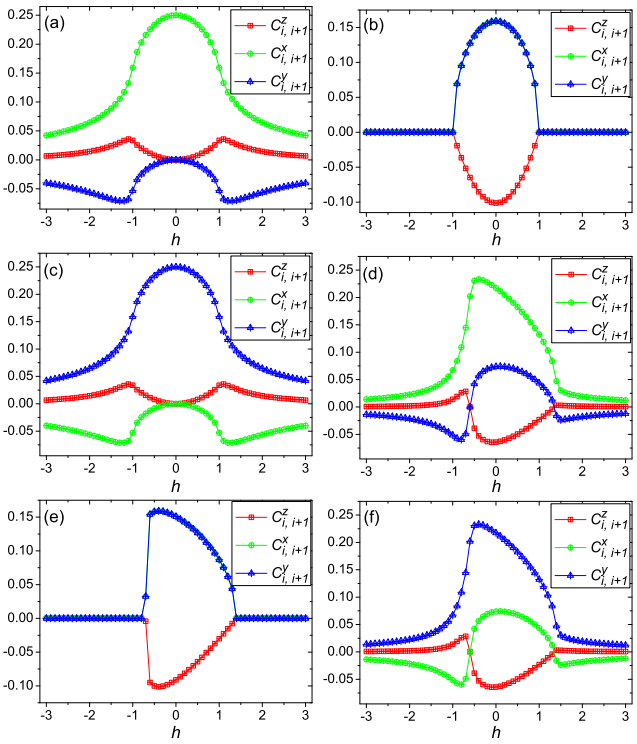


FIG. 10: (color online) The nearest neighbors spin-spin correlations $C^x_{i,i+1}$, $C^y_{i,i+1}$, and $C^z_{i,i+1}$ as functions of $h$, with the fixed parameters (a): $\gamma = 1, \delta = 0$; (b): $\gamma = 0, \delta = 0$; (c): $\gamma = -1, \delta = 0$; (d): $\gamma = 0.3, \delta = 0.4$; (e): $\gamma = 0, \delta = 0.4$; (f): $\gamma = -0.3, \delta = 0.4$.

The spin-spin correlation functions can be derived by using the similar method for the transverse field XY spin

model (see Refs. [20] and Ref. [71]), and we can obtain

$$\begin{aligned} C^x_{i,i+r} &= \langle S^x_0 S^x_r\rangle - \langle S^x_0\rangle\langle S^x_r\rangle \\ &= \frac{1}{4}\begin{vmatrix} G_{-1} & G_{-2} & \cdot & G_{-r} \\ G_0 & G_{-1} & \cdot & G_{-r+1} \\ \vdots & \vdots & \ddots & \vdots \\ G_{r-2} & G_{r-3} & \cdot & G_{-1} \end{vmatrix}, \\ C^y_{i,i+r} &= \langle S^y_0 S^y_r\rangle - \langle S^y_0\rangle\langle S^y_r\rangle \\ &= \frac{1}{4}\begin{vmatrix} G_1 & G_0 & \cdot & G_{-r+2} \\ G_2 & G_1 & \cdot & G_{-r+3} \\ \vdots & \vdots & \ddots & \vdots \\ G_r & G_{r-1} & \cdot & G_1 \end{vmatrix}, \\ C^z_{i,i+r} &= \langle S^z_0 S^z_r\rangle - \langle S^z_0\rangle\langle S^z_r\rangle = -\frac{1}{4}G_r G_{-r}, \end{aligned} \quad (23)$$

where the expectation values $\langle\ \rangle$ are taken in the ground state (at zero temperature) or in the canonical ensemble (at finite temperature), and the Green function $G_r$ at finite temperature is given by

$$\begin{aligned} G_r(\beta) &= \frac{1}{\pi}\int_0^\pi (h+\cos k-\delta\cos 2k)\cos kr\frac{\tanh\left(\frac{1}{2}\beta\Lambda_k\right)}{\Lambda_k} \\ &\quad -\gamma\sin k\sin kr\frac{\tanh\left(\frac{1}{2}\beta\Lambda_k\right)}{\Lambda_k}dk, \end{aligned} \quad (24)$$

where $\beta = k_BT$ and the energy spectrum $\Lambda_k = \sqrt{(h+\cos k-\delta\cos 2k)^2+\gamma^2\sin^2 k}$. Meanwhile, the Green function $G_r$ at zero temperature can be obtained by setting $\tanh(\beta\Lambda_k/2)=1$, that is,

$$G_r = \frac{1}{\pi}\int_0^\pi \frac{(h+\cos k-\delta\cos 2k)\cos kr-\gamma\sin k\sin kr}{\sqrt{(h+\cos k-\delta\cos 2k)^2+\gamma^2\sin^2 k}}dk. \quad (25)$$

The nearest neighbors spin-spin correlation functions at zero temperature as functions of $h$ with different Hamiltonian parameters $\gamma$ and $\delta$ have been shown in Fig. 10.

On the other hand, the Euler number of the system can be expressed as (see Eq. (16))

$$\chi = \frac{1}{2\pi}\int_{1\mathrm{Bz}} 4\sqrt{\mathcal{G}_{kk}\cdot\mathcal{G}_{\varphi\varphi}}dkd\varphi, \quad (26)$$

where the Riemannian metric $\mathcal{G}_{kk}$ and $\mathcal{G}_{\varphi\varphi}$ are given by Eq. (8). Considering Eqs. (23), (25), and (8), we have

$$\frac{1}{2\pi}\iint \sin k\sqrt{\mathcal{G}_{\varphi\varphi}}dkd\varphi = \frac{\pi}{4}\left(C^x_{i,i+1}-C^y_{i,i+1}\right). \quad (27)$$

By a similar way, the metric component $\mathcal{G}_{kk}$ and the Euler number can also be expressed in some combination of the spin-spin correlation functions.

In Figs. 11(a), 11(b), and 11(c), we show the correlation functions $C^x_{i,i+1}$, $C^x_{i,i+1}$, and $C^z_{i,i+1}$ as the functions of the transverse field $h$ with the Hamiltonian parameters $\gamma = 0.3$, and $\delta = 0,\ 0.5,\ 1$. In Figs. 11(d), 11(e), and 11(f), we show the correlation functions as the functions of the three-site spin coupling coefficient $\delta$ with the Hamiltonian parameters $\gamma = 0.3$, and $h = 0,\ 0.5,\ 1$. As shown in Fig. 11, the three-site spin coupling coefficient $\delta$ will affect the behavior of the spin-spin correlation functions. Meanwhile, the critical points of the system will be moved to $h = \delta \pm 1$ where the energy gap will be closed, and this can be witnessed by the Euler number of the band.

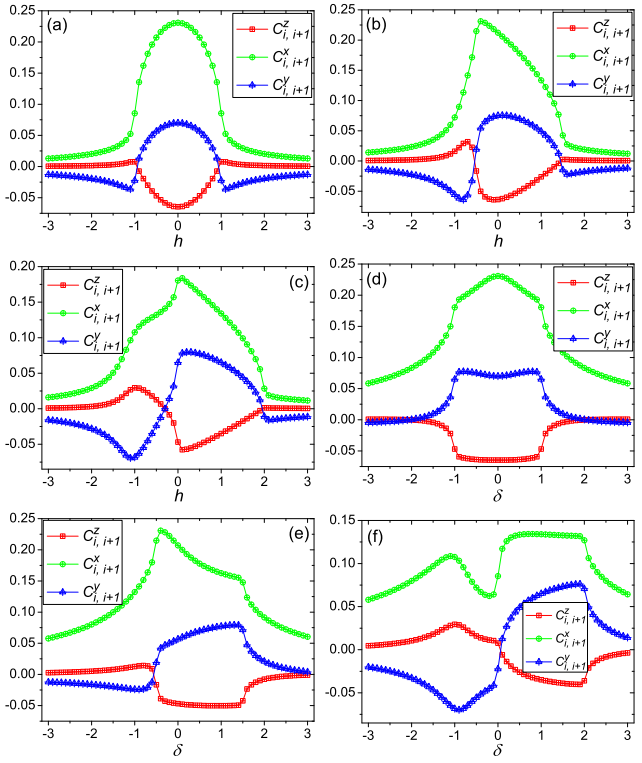


FIG. 11: (color online) The spin-spin correlations $C^x_{i,i+1}$, $C^y_{i,i+1}$, and $C^z_{i,i+1}$ as the function of $h$ with the fixed parameters $\gamma = 0.3$, and (a): $\delta = 0$; (b): $\delta = 0.5$; (c): $\delta = 1$; The spin-spin correlations $C^x_{i,i+1}$, $C^y_{i,i+1}$, and $C^z_{i,i+1}$ as the function of $\delta$ with the fixed parameters $\gamma = 0.3$, and (d): $h = 0$; (e): $h = 0.5$; (f): $h = 1$.

## V. CONCLUSIONS

In summary, we study the Euler number index of the Bloch band in a transverse field XY spin-1/2 chain with multi-site spin couplings. This approach is based on the topological characterization from the Gauss-Bonnet theorem on a 2D closed Bloch states manifold in the first Brillouin zone, where the Riemannian structure of the Bloch band is established by the geometric tensor in the crystal momentum space. For a local geometric witness to the quantum phase transitions, we introduce the cyclic quantum distance of the Bloch band and show the Riemannian metric on the Bloch states manifold can be relate to a

corresponding ground-state quantum distance in the parameter space. Finally, we derive the Euler characteristic number of the Bloch band analytically via the Gauss-Bonnet theorem on the 2D Bloch states manifold in the first Brillouin zone. We show that the ferromagnetic-paramagnetic quantum phase transition in this model is topologically different in the Bloch band's Euler number index. We also give a general formula of the Euler number for the 1D or 2D two-band systems, which reveals its essential relation to the first Chern number of the band insulators.

## VI. ACKNOWLEDGMENTS

The author would like to thank Han Zhang for helpful discussions and thank the referee for the constructive comments which helped to improve the manuscript. This work was supported by the Special Foundation for Theoretical Physics Research of NSFC under Grant No. 11347131 and NSFC under Grant No. 11404023.

[1] R. B. Laughlin, Phys. Rev. B **23**, 5632 (1981).
[2] D. J. Thouless, M. Kohmoto, M. P. Nightingale and M. den Nijs, Phys. Rev. Lett. **49**, 405 (1982).
[3] Q. Niu and D. J. Thouless, J. Phys. A **17**, 2453 (1984).
[4] D. J. Thouless, Phys. Rev. B **27**, 6083 (1983).
[5] Q. Niu, Phys. Rev. Lett. **64**, 1812 (1990).
[6] C. L. Kane and E. J. Mele, Phys. Rev. Lett. **95**, 146802 (2005); **95**, 226801 (2005).
[7] L. Fu, C. L. Kane, and E. J. Mele, Phys. Rev. Lett. **98**, 106803 (2007).
[8] S. S. Lee and S. Ryu, Phys. Rev. Lett. **100**, 186807 (2008).
[9] M. Z. Hasan and C. L. Kane, Rev. Mod. Phys. **82**, 3045 (2010).
[10] X. L. Qi and S. C. Zhang, Rev. Mod. Phys. **83**, 1057 (2011).
[11] E. Tang, J. W. Mei, and X. G. Wen, Phys. Rev. Lett. **106**, 236802 (2011).
[12] K. Sun, Z. Gu, H. Katsura, and S. Das Sarma, Phys. Rev. Lett. **106**, 236803 (2011).
[13] T. Neupert, L. Santos, C. Chamon, and C. Mudry, Phys. Rev. Lett. **106**, 236804 (2011).
[14] S. Sachdev, *Quantum Phase Transitions* (Cambridge University Press, Cambridge, UK, 1999).
[15] S. L. Sondhi, S. M. Girvin, J. P. Carini, and D. Shahar, Rev. Mod. Phys. **69**, 315 (1997).
[16] M. Vojta, Rep. Prog. Phys. **66**, 2069 (2003).
[17] I. Bengtsson and K. Zyczkowski, *Geometry of Quantum States: An Introduction to Quantum Entanglement* (Cambridge University Press, Cambridge, 2006).
[18] G. Ortiz, in *Understanding in Quantum Phase Transitions* edited by L. Carr (Taylor & Francis, Boca Raton, 2010).
[19] A. Osterloh, L. Amico, G. Falci, and R. Fazio, Nature (London) **416**, 608 (2002).
[20] T. J. Osborne and M. A. Nielsen, Phys. Rev. A **66**, 032110 (2002).
[21] G. Vidal, J. I. Latorre, E. Rico, and A. Kitaev, Phys. Rev. Lett. **90**, 227902 (2003).
[22] S. J. Gu, S. S. Deng, Y. Q. Li, H. Q. Lin, Phys. Rev. Lett. **93**, 086402 (2004).
[23] F. Verstraete, M. A. Martin-Delgado, and J. I. Cirac, Phys. Rev. Lett. **92**, 087201 (2004).
[24] A. Kitaev and J. Preskill, Phys. Rev. Lett. **96**, 110404 (2006).
[25] M. Levin and X. G. Wen, Phys. Rev. Lett. **96**, 110405 (2006).
[26] H. Ollivier and W. H. Zurek, Phys. Rev. Lett. **88**, 017901 (2001).
[27] A. Datta, A. Shaji, and C. M. Caves, Phys. Rev. Lett. **100**, 050502 (2008).
[28] S. Campbell, L. Mazzola, G. De Chiara, et. al. , New J. Phys. **15**, 043033 (2013).
[29] P. Zanardi and N. Paunkovi′c, Phys. Rev. E **74**, 031123 (2006).
[30] W. L. You, Y. W. Li and S. J. Gu, Phys. Rev. E **76**, 022101 (2007).
[31] S. J. Gu, Int. J. Mod. Phys. B, **24**, 4371 (2010).
[32] S. Chen, L. Wang, S. J. Gu and Y. Wang, Phys. Rev. E **76**, 061108 (2007).
[33] S. Yang, S. J. Gu, C. P. Sun and H. Q. Lin, Phys. Rev. A **78**, 012304 (2008).
[34] J. H. Zhao and H. Q. Zhou, Phys. Rev. B **80**, 014403 (2009).
[35] M. M. Rams and B. Damski, Phys. Rev. A **84**, 032324 (2011).
[36] M. Thakurathi, D. Sen, and A. Dutta, Phys. Rev. B **86**, 245424 (2012).
[37] B. Damski, Phys. Rev. E **87**, 052131 (2013).
[38] Y. Nishiyama, Phys. Rev. E **88**, 012129 (2013).
[39] M. V. Berry, Proc. R. Soc. London A **392**, 45 (1984).
[40] B. Simon, Phys. Rev. Lett. **51**, 2167 (1983).
[41] R. Resta, Rev. Mod. Phys. **66**, 899 (1994).
[42] D. Xiao, M. C. Chang, and Q. Niu, Rev. Mod. Phys. **82**, 1959 (2010).
[43] A. C. M. Carollo and J. K. Pachos, Phys. Rev. Lett. **95**, 157203 (2005).
[44] A. Hamma, arXiv: quant-ph/0602091.
[45] S. L. Zhu, Phys. Rev. Lett. **96**, 077206 (2006).
[46] Y. Q. Ma and S. Chen, Phys. Rev. A **79**, 022116 (2009).
[47] T. Hirano, H. Katsura, and Y. Hatsugai, Phys. Rev. B **77**, 094431 (2008); Y. Hatsugai, New J. Phys. **12**, 065004 (2010).
[48] T. Fukui and T. Fujiwara, J.Phys.Soc.Jpn. **78**, 093001 (2009).
[49] Y. Q. Ma, et. al., EPL **100**, 60001 (2012).
[50] J. P. Provost and G. Vallee, Commun. Math. Phys. **76**. 289 (1980).
[51] M. V. Berry, in *Geometric Phases in Physics*, edited by A. Shapere and F. Wilczek (World Scientific, Singapore, 1989).
[52] R. Resta, Phys. Rev. Lett. **95**, 196805 (2005).
[53] L. Campos Venuti and P. Zanardi, Phys. Rev. Lett. **99**, 095701 (2007).

[54] P. Zanardi, P. Giorda and M. Cozzini, Phys. Rev. Lett. **99**, 100603 (2007).

[55] Y. Q. Ma, S. Chen, H. Fan, and W. M. Liu, Phys. Rev. B **81**, 245129 (2010).

[56] S. Matsuura and S. Ryu, Phys. Rev. B **82**, 245113 (2010).

[57] F. D. M. Haldane, Phys. Rev. Lett. **107**, 116801 (2011).

[58] T. Neupert, C. Chamon, and C. Mudry, Phys. Rev. B **87**, 245103 (2013).

[59] J. Zak, Phys. Rev. Lett. **62**, 2747 (1989).

[60] M. Atala, M. Aidelsburger, J. T. Barreiro, D. Abanin, T. Kitagawa, E. Demler, and I. Bloch, Nature Phys. **9**, 795 (2013).

[61] Y. Q. Ma, S. J. Gu, S. Chen, H. Fan, and W. M. Liu, arXiv:1202.2397; EPL **103**, 10008 (2012).

[62] M. Kolodrubetz, V. Gritsev, A. Polkovnikov, Phys. Rev. B **88**, 064304 (2013).

[63] P. Lou, W. C. Wu, and M. C. Chang, Phys. Rev. B **70**, 064405 (2004).

[64] A. A. Zvyagin and G. A. Skorobagat'ko, Phys. Rev. B **73**, 024427 (2006); A. A. Zvyagin, Phys. Rev. B **80**, 014414 (2009).

[65] J. H. H. Perk, and H. A. Yang, J. Stat. Phys. **135**, 599 (2009).

[66] W. W. Cheng and J. M. Liu, Phys. Rev. A **82**, 012308 (2010).

[67] Note the Riemannain metric of the Bloch states $u_\pm\left(k,\varphi\right)$ is given by $\mathcal{G}^{\pm}_{k\varphi} = \frac{1}{2}\langle\partial_k u_\pm|\partial_\varphi u_\pm\rangle + \frac{1}{2}\langle\partial_\varphi u_\pm|\partial_k u_\pm\rangle - \langle\partial_k u_\pm|u_\pm\rangle\langle u_\pm|\partial_\varphi u_\pm\rangle$, and it can be verified that here $\mathcal{G}^{+}_{k\varphi} = \mathcal{G}^{-}_{k\varphi}$, so we can denote the metric as $\mathcal{G}_{k\varphi}$ conveniently.

[68] A. P. Schnyder, S. Ryu, A. Furusaki, and A. W. W. Ludwig, Phys. Rev. B **78**, 195125 (2008); AIP Conf. Proc. **1134**, 10 (2009); A. Kitaev, *ibid.* **1134**, 22 (2009); S. Ryu, A. P. Schnyder, A. Furusaki, and A. W. W. Ludwig, New J. Phys. **12**, 065010 (2010).

[69] S. Tewari, and J. D. Sau, Phys. Rev. Lett. **109**, 150408 (2012).

[70] N. Marzari and D. Vanderbilt, Phys. Rev. B **56**, 12847 (1997).

[71] S. Suzuki, J. Inoue, and B. K. Chakrabarti, *Quantum Ising Phases and Transitions in Transverse Ising Models*, Vol. 862 (Lecture Notes in Physics, Springer, Berlin, 2013).